HHS Public Access

Author manuscript

Dev Dyn. Author manuscript; available in PMC 2024 March 01.

Published in final edited form as:

Dev Dyn. 2023 March ; 252(3): 415–428. doi:10.1002/dvdy.550.

Novel roles for RNA binding proteins *squid, hephaesteus*, and *Hrb27C* in *Drosophila* oogenesis

Danielle S. Finger,

Anna E. Williams,

Vivian V. Holt,

Elizabeth T. Ables*

Department of Biology, East Carolina University, Greenville, NC 27858, USA.

Abstract

Background: Reproductive capacity in many organisms is maintained by germline stem cells (GSCs). A complex regulatory network influences stem cell fate, including intrinsic factors, local signals, and hormonal and nutritional cues. Post-transcriptional regulatory mechanisms ensure proper cell fate transitions, promoting germ cell differentiation to oocytes. As essential RNA binding proteins with constitutive functions in RNA metabolism, heterogeneous nuclear ribonucleoproteins (hnRNPs) have been implicated in GSC function and axis specification during oocyte development. HnRNPs support biogenesis, localization, maturation, and translation of nascent transcripts. But whether individual hnRNPs specifically regulate GSC function has yet to be explored.

Results: We demonstrate that hnRNPs are expressed in distinct patterns in the *Drosophila* germarium. We show that three hnRNPs, *squid, hephaestus*, and *Hrb27C* are cell-autonomously required in GSCs for their maintenance. Although these hnRNPs do not impact adhesion of GSCs to adjacent cap cells, *squid* and *hephaestus* (but not *Hrb27C*) are necessary for proper BMP signaling in GSCs. Moreover, *Hrb27C* promotes proper GSC proliferation, whereas *hephaestus* promotes cyst division.

Conclusions: We find that hnRNPs are independently and intrinsically required in GSCs for their maintenance in adults. Our results support the model that hnRNPs play unique roles in stem cells essential for their self-renewal and proliferation.

SUMMARY STATEMENT

Heterogeneous ribonucleoproteins encoded by *squid, hephaestus*, and *Hrb27C* are necessary for germline stem cell maintenance in the *Drosophila* ovary.

***Corresponding author**: Elizabeth T. Ables, East Carolina University, Department of Biology, 1001 E. 10th St., Mailstop 552, 553 Science & Technology Building, Greenville, NC 27858, Office phone: 252-328-9770, ablese@ecu.edu.

AUTHOR CONTRIBUTIONS

D.S.F. and E.T.A. conceived and designed experiments, analyzed data, interpreted results, and wrote the manuscript. D.S.F. performed the experiments and managed the project. A.E.W. and V.V.H. assisted with experiment planning, collected data, and assisted in figure preparation. All authors provided critical feedback and helped shape the research, analysis, and manuscript.

COMPETING INTERESTS

The authors declare no competing conflicts of interest.

Keywords

germ cell; oocyte; hnRNP; oogenesis

INTRODUCTION

Stem cells are critical for tissue homeostasis and cellular diversity in developing and mature organs. Many stem cells divide asymmetrically, balancing long-term stem cell self-renewal with the production of progenitor cells that differentiate into functionally specialized cells[1–3]. To ensure tissue integrity and proper organ function, stem cell self-renewal and proliferation must be tightly regulated. As stem cell decline contributes to age-related tissue degeneration[4–6], understanding how stem cell activity is controlled may offer new strategies for optimization of tissue repair and regeneration *in vivo*.

The *Drosophila melanogaster* ovary is a robust model system with which to elucidate the molecular mechanisms controlling stem cell function. Ovaries are comprised of 14–16 ovarioles filled with maturing egg chambers or follicles, each of which will ultimately develop into a single oocyte (Figure 1A)[7]. Germline stem cells (GSCs) reside at the most anterior region of the ovariole (called the germarium; Figure 1B). Asymmetric division of the GSC perpendicular to the cap cells produces another GSC and a cystoblast committed to differentiation. The cystoblast mitotically divides four times with incomplete cytokinesis to form an interconnected 16-cell germline cyst. One cell of the cyst differentiates to form the oocyte, while the remaining cells become nurse cells, which ultimately load the oocyte with maternal factors essential for embryogenesis (Figure 1B).

GSCs are regulated by a complex network of paracrine and endocrine signaling mechanisms that maintain their self-renewal and proliferation in concert with intrinsic controls[8–10]. GSCs are physically connected via adherens junctions to adjacent somatic cap cells (Figure 1B), which secrete the bone morphogenetic protein (BMP) ligands Decapentaplegic (Dpp) and Glass bottom boat (Gbb)[11,12]. Upon activation, BMP receptors Punt (Put) and Thickveins (Tkv) on GSCs suppress differentiation via activation of Mothers against decapentaplegic (Mad), which transcriptionally represses Bag of marbles (Bam), a primary differentiation factor[13–15]. Translational control of differentiation factors is also critical for regulating GSC self-renewal and cystoblast differentiation[16,17]. Alternative splicing, RNA modification, and ribosome biogenesis each control the output of gene expression in the germline to modulate cell fate transitions. Thus, uncovering the specific roles of proteins that post-transcriptionally regulate gene expression is critical to understanding how GSCs are maintained in a self-renewing proliferative state.

Heterogeneous nuclear ribonucleoproteins (hnRNPs) are a large and diverse family of RNA binding proteins that act as essential regulators of RNA metabolism, localization, and stability[18–20]. At least 14 hnRNPs are encoded in the *Drosophila* genome[20,21]. HnRNPs function constitutively as RNA packaging proteins and in RNA biogenesis, but also function in a regulatory capacity by binding specific RNAs and interacting with other regulatory factors, including other hnRNPs[19,21,22]. Aberrant germline phenotypes, including dorsalized eggs and female sterility, were among the first biological processes attributed to mutations

in *Drosophila* hnRNPs[23–30]. For example, Heterogeneous nuclear ribonucleoprotein at 98DE (Hrb98DE) stabilizes *E-cadherin* mRNA to promote stem cell adhesion and oocyte location within cysts[31], while hnRNPs Squid (Sqd), Heterogeneous nuclear ribonucleoprotein at 27C (Hrb27C), Glorund, Hephaestus (Heph), and Syncrip (Syp) spatially restrict mRNAs in the *Drosophila* oocyte to establish the embryonic body axes[20]. HnRNPs are thought to play essential roles in stem cell maintenance and progenitor cell differentiation in mammals[32]. Moreover, *Hrb27C* was identified as a potential regulator of GSC maintenance in large-scale genetic screens, suggesting that additional hnRNPs other than Hrb98DE are also active in GSCs[33,34]. Yet while phenotypic reports of *Hrb27C* and *sqd* mutants hinted at potential function in GSCs or the early germline[30], roles for hnRNPs in mitotically dividing germ cells in *Drosophila* have remained largely unexplored.

In this study, we investigated whether *Hrb27C* or other hnRNP family members contribute to GSC maintenance and/or early germ cell development in *Drosophila*. We identified unique protein localization patterns for six hnRNPs in the *Drosophila* germarium, which suggest cell type-specific functions for hnRNPs in oogenesis. We also uncovered novel roles in oogenesis for the hnRNP family members *Hrb27C*, *sqd*, and *heph*. Using spatially and temporally controlled loss-of-function analyses, our data suggest that *Hrb27C*, *sqd*, and *heph* are independently and intrinsically required in GSCs for their maintenance. In contrast to the known mechanism of action of related hnRNP *Hrb98DE*, depletion of *Hrb27C*, *sqd* or *heph* did not impact adhesion of GSCs to cap cells; however, loss of *sqd* or *heph*, but not *Hrb27C*, resulted in reduced BMP signal activation in GSCs. We also provide evidence that *Hrb27C* promotes GSC proliferation, while *heph* promotes cyst division. Taken together, these data support the hypothesis that hnRNPs bind a non-overlapping set of transcripts in GSCs and are essential in GSCs and their immediate daughters to support oogenesis in adult females.

RESULTS

hnRNPs are differentially expressed in the germarium.

To explore whether specific hnRNPs could function in the earliest stages of oocyte development, we used available protein trap transgenes and antibodies in wild-type ovaries to assess the cellular expression and subcellular localization of hnRNPs. We focused on the germarium, which is the anterior-most portion of the *Drosophila* ovariole and the location of GSCs and mitotically-dividing germ cells (Figure 1A–B). We performed immunofluorescence for green fluorescent protein (GFP) on ovaries from young, well-fed females harboring transgenes *Hrb27C::GFP* (Figure 1C), *sqd::GFP* (Figure 1D), *heph::GFP* (Figure 1E), *nonA::GFP* (Figure 1F), or *Hrb87F::GFP* (Figure 1G), which use endogenous gene loci to drive expression of hnRNP proteins tagged with GFP. We co-localized GFP with antibodies against Hu li tai shao (Hts), an adducin-like protein which localizes to fusomes in germ cells and plasma membranes in follicle cells, and antibodies against LaminC (LamC), which is highly expressed in the nuclear lamina of cap cells (Figure 1C–G). This combination of antibodies allowed us to visualize germline and somatic cells in the germarium based on their location and the abundance and/or localization of Hts and LamC. We detected cytoplasmic GFP in germ cells in ovaries from *Hrb27C::GFP*, *sqd::GFP*, and *heph::GFP* females -in distinct, yet overlapping, regions in the germarium (Figure 1C–

E). Expression of *Hrb27C::GFP* was particularly strong in 8-cell cysts (Figure 1C), while expression of *heph::GFP* was stronger in mitotically dividing cysts than in 16-cell cysts (Figure 1E). GFP was localized prominently in germ cell nuclei in ovaries from *nonA::GFP* and *Hrb87F::GFP* females (Figure 1F–G).

We also observed expression of hnRNPs in somatic cells. GFP was detected in cap cells in *nonA::GFP* and *sqd::GFP* germaria (Figure 1D, F), while *Hrb27C::GFP* and *heph::GFP* were expressed primarily in follicle cells (Figure 1C, E). *Hrb87F::GFP* was observed at much higher levels in somatic escort and follicle cells than in germ cells (Figure 1G). Similarly, we also localized Syp protein in the germarium using an available antibody[35] on wild type female flies. We found Syp exclusively expressed in the cytoplasm of somatic cells in the germarium, including cap cells, escort cells, and follicle cells (Figure 1H). These data indicate that hnRNPs are expressed in cell type-specific patterns and localize in either cytoplasm or nuclei in germ cells and surrounding somatic cells at the earliest stages of oocyte development.

Three HnRNPs are independently and autonomously required in GSCs for their maintenance.

The distinct expression patterns of hnRNPs in the germline and somatic cells of the germarium suggests that these proteins may have at least partially independent roles in germ cells. Indeed, prior studies indicate that *sqd*, *Hrb27C*, and *heph* are present in a ribonucleoparticle complex that represses translation of *oskar* mRNA in late oogenesis, aiding in oocyte axis patterning[20]. Yet their expression in GSCs and mitotically dividing germ cells suggest that these hnRNPs have additional, earlier functions other than oocyte axis patterning in late oogenesis. Having previously identified *Hrb27C* in genetic screens for novel regulators of GSC maintenance[33,34], we hypothesized that one function of *sqd*, *Hrb27C*, and *heph* might be to promote GSC self-renewal. To test this hypothesis, we used *Flippase/Flippase Recognition Target* (*Flp/FRT*)-mediated mosaic recombination with a negative labeling system and available *FRT*-containing loss-of-function mutants to inactivate the function of *Hrb27C*, *sqd*, or *heph* in GSCs specifically in adults (Figure 2A)[36]. (Despite their expression in GSCs, we were not able to further examine potential roles for *nonA* or *Hrb87F* in germ cells using this technique, as suitable genetic stocks in the *FRT* background could not be attained.) *Flp/FRT*-mediated mosaicism allowed us to lineage-trace clonal populations of homozygous mutant cells in otherwise heterozygous animals. An *FRT* site lies proximal to a mutation in a gene of interest in trans to another *FRT* chromosome arm carrying the corresponding wild-type allele linked to a GFP marker (Figure 2A). Flp catalyzes mitotic recombination between the *FRT* sites in dividing cells, leading to the formation of clones of homozygous mutant cells. We used a heat-shock-promoter driven *Flp* transgene that expresses the Flp recombinase in response to high temperature, and thus mediates recombination in a time-controlled manner. This system is particularly useful for the dissection of gene function in GSCs because it allows the experimenter to genetically label homozygous mutant cells and follow their “output” over time, as all daughter cells generated from the homozygous mutant GSC are GFP-negative.

In this assay, GSCs and their daughter cells carrying homozygous mutations in *sqd* (Figure 2C), *heph* (Figure 2D), or *Hrb27C* (Figure 2E) were recognized by loss of GFP in mosaic germaria. We specifically selected null or strong hypomorphic alleles of *sqd* (*sqd*^{ix50} and *sqd*^{ix77}), *heph* (*heph*^{e1} and *heph*^{e2}) and *Hrb27C* (*Hrb27C*^{F680}, *Hrb27C*^{k02814}, and *Hrb27C*^{f04375}) for our analyses, each of which has been previously described[23,28,37,38]. Germaria were analyzed eight days after clone induction, allowing negatively labeled cystoblasts/cysts to be cleared from germaria and ensuring that GFP-negative cysts originated from a negatively labeled GSC[36]. In control "mock mosaic" germaria, where all cells are wild-type, GFP-negative GSCs were nearly always accompanied by GFP-negative cystoblasts/cysts, resulting in very few germaria with a GSC loss phenotype (Figure 2B, F) and indicating that these GSCs self-renew and produce differentiating progeny. In contrast, significant percentages of *sqd*, *heph*, and *Hrb27C* mutant mosaic germaria contained GFP-negative cysts without an accompanying GFP-negative GSC, evidence that the mutant GSC produced some progeny, but had reduced capacity to be maintained in the niche (Figure 2C–F). Although we cannot rule out possible roles for these hnRNPs in somatic cells in the germarium, these data demonstrate that *sqd*, *heph*, and *Hrb27C* are independently and autonomously necessary in GSCs for their maintenance in the niche.

Technical limitations prevented us from specifically inactivating *Hrb87F* function in GSCs using the *FLP/FRT* technique. A report describing decreased female fecundity in *Df(3R)Hrb87F* mutants[39], however, prompted us to investigate whether it is also necessary for GSC maintenance. Female homozygous *Df(3R)Hrb87F* mutants (see Experimental Procedures) survived to adulthood, but had multiple defects in oogenesis and were sterile[39]. We observed a more rapid rate of decline of GSCs per germarium in female homozygous *Df(3R)Hrb87F* mutants as compared to heterozygous sibling controls (Figure 2I). While we cannot determine from this assay whether *Hrb87F* functions in the GSCs or the soma or both, this data supports the hypothesis that *Hrb87F* also contributes to the proper maintenance of GSCs as flies age.

Hrb27C is necessary for GSC proliferation, while *heph* is necessary for timely cyst division.

Apparent loss of GSCs in our *Flp/FRT* lineage tracing assay could be compounded by defects in cyst division. To measure the rate of cyst production, we examined mosaic germaria with both wild-type (GFP+) and hnRNP mutant (GFP-) cysts, and quantified the number of cysts at each stage of mitotic division according to the morphology of the fusome, a specialized organelle that branches with each cyst division (Figure 3A–E)[40,41]. The proportion of mutant and neighboring GFP-positive cystoblasts/cysts at each mitotic division was equivalent in *sqd*^{ix50} and *Hrb27C*^{rF680} mutant mosaic germaria (Figure 3E). In contrast, although we observed *heph*^{e2} mutant cysts at all stages of mitotic division (see Figure 2D, for example), *heph*^{e2} mutant 4-, 8-, and 16-cell cysts were under-represented in mosaic germaria (Figure 3B, E). To further assess cyst division rates, we then compared the number of GFP− cysts per GSC to the number of GFP+ cysts per GSC, and calculated cyst division rate as a ratio of the two values. If the rate of cyst division is equivalent between mutant (GFP-) cysts and adjacent wild-type (GFP+) cysts, then the cyst division ratio should roughly equal 1.0. Indeed, this was the case for *Hrb27C*^{F680} and *sqd*^{ix50} mutant

mosaic germaria, which had cyst division ratios of 1.2 (n = 39 germaria; 544 cysts) and 0.93 (n = 23 germaria; 300 cysts), respectively. In contrast, the cyst division ratio of *heph*^{e2} mutant mosaic germaria equaled 0.48 (n = 38 germaria; 373 cysts), indicating that *heph* mutant cysts divide slower than their wild-type counterparts (see Figure 3B as an example). Moreover, we found no evidence of caspase-mediated apoptosis in *sqd*^{ix50} (Figure 3C), *heph*^{e2} (Figure 3B), or *Hrb27C*^{F680} (Figure 3D) mutant mosaic germaria, suggesting that GSCs or cysts are not lost due to premature cell death. These data suggest that *heph*, but not *sqd* or *Hrb27C*, is specifically necessary for timely cyst division.

The rate of cyst production is also dependent on the rate of GSC proliferation. To test whether hnRNP mutant GSCs progressed through the cell cycle at equivalent rates to wild-type GSCs, we measured the percentage of GFP-negative GSCs that incorporated the thymidine analog EdU in mosaic germaria (Figure 3F–J). In mock mosaic germaria (where all cells are wild-type), 10–12% of GFP-negative GSCs are labeled with EdU during a one-hour pulse (Figure 3F, J). We did not observe statistically significant differences in rates of proliferation in *sqd*^{ix50} (Figure 3G, J) or *heph*^{e2} (Figure 3H, J) mutant GSCs versus mock GFP-negative control GSCs. In contrast, significantly fewer *Hrb27C*^{rF680} mutant GSCs incorporated EdU versus controls (Figure 3I–J), indicating that *Hrb27C* specifically promotes GSC cell cycle progression. Taken together, these results argue against a general germ cell dysfunction in hnRNP mutant cells, but instead support the model that *Hrb27C*, *heph*, and *sqd* control distinct cellular processes in GSCs and dividing germ cells.

Loss of *heph*, *sqd*, or *Hrb27C* does not impair GSC adhesion to cap cells.

E-cadherin localizes at the interface between cap cells and GSCs and is necessary for GSC self-renewal[12]. We therefore hypothesized that *Hrb98DE*, *sqd, heph*, and *Hrb27C* promote GSC self-renewal by stabilizing the physical attachment of GSCs to the stem cell niche by adherens junctions. To test whether loss of *Hrb27C*, *heph*, or *sqd* abrogated E-cadherin expression, we performed immunofluorescence for E-cadherin in *sqd*, *heph*, and *Hrb27C* mosaic germaria (Figure 4A, C, E). This allowed us to directly compare E-cadherin mean fluorescence intensity at the cap cell-GSC interface between hnRNP mutant GSCs and adjacent wild-type GSCs (Figure 4B, D, F). We found, however, that E-cadherin expression in *sqd*^{ix50} (Figure 4A–B), *heph*^{e2} (Figure 4C–D), or *Hrb27C*^{rF680} mutant GSCs (Figure 4E–F) was comparable to adjacent wild-type (GFP+) GSCs. These data indicate that loss of *sqd*, *heph*, or *Hrb27C* independently does not deplete E-cadherin levels at the GSC/cap cell interface, suggesting that impaired maintenance of *sqd, heph*, and *Hrb27C* mutant GSCs is not due to loss of a physical attachment to the niche.

heph and *sqd* mutant GSCs have a reduced response to BMP signals.

BMP signaling via Mad is necessary to repress transcription of the differentiation factor *bam* in GSCs, thus suppressing their differentiation[13,15]. We therefore wanted to address whether *sqd*, *heph*, or *Hrb27C* mutant GSCs might prematurely express Bam, potentially causing their differentiation. Unfortunately, we were unable to successfully visualize Bam anti-sera in combination with our mosaic clonal markers, and technical limitations of the Flp/FRT mosaic system prevented us from monitoring Bam transgenic reporter lines in the context of *sqd*, *heph*, or *Hrb27C* mosaic germaria. We therefore sought an alternative

strategy to deplete hnRNPs from GSCs and their immediate daughters. In combination with the bipartite *Upstream Activating Sequence* (*UAS*) / Gal4 transactivation system, RNA interference (RNAi) is a powerful, cell-specific tool to deplete target mRNA from cells[42]. We tested available *UAS-RNAi* transgenic strains for *Hrb27C* or *heph* by driving the RNAi under the control of germline-specific Gal4 transgenes, but these lines did not impact oogenesis, likely because the transgenes are targeted for destruction[43]. We did, however, identify two *UAS-RNAi* transgenic strains, sqd^{GL} and sqd^{HMC}, that target *sqd* and phenocopied *sqd* null mutant phenotypes, including GSC depletion (Figure 5A) and egg dorsalization (Figure 5B)[23,24]. We therefore focused our analyses on the sqd^{GL} RNAi line, which produced the strongest phenotypes, and asked whether *sqd*-depleted GSCs prematurely induced Bam expression. We monitored Bam protein expression using a transgene (*Bam-sfGFP*) carrying a fosmid genomic fragment wherein *bam* was fused at the C-terminus with green fluorescent protein (GFP)[44]. In driver-only control germaria, Bam-sfGFP is absent from GSCs, but expressed in differentiating 2-cell and 4-cell cysts (Figure 5C; n = 68 germaria). An identical expression pattern was previously reported using Bam anti-sera[14]. Similarly, Bam-sfGFP was undetectable in GSCs in *sqd*-depleted germaria (Figure 5D; n = 74 *nos-Gal4::VP16>*sqd^{HMC} germaria, n = 62 *nos-Gal4::VP16>*sqd^{GL} germaria). We also noted, however, that GSC number in *sqd* RNAi lines did not decrease substantially as the flies aged (i.e. from 3- to 12-days after eclosion) (Figure 5A). This suggests that the level of *sqd* knock-down is sufficient in the RNAi background to reduce, but not completely abolish, the ability of GSCs to self-renew. It is therefore not clear whether *bam* expression is not affected by depletion of *sqd*, or whether the levels of *sqd* have not been sufficiently reduced in the RNAi experimental model to fully de-repress *bam*.

To further test whether premature differentiation contributed to the loss of *sqd, heph*, and *Hrb27C* mutant GSCs from the niche, we then asked whether hnRNP mutant GSCs could properly respond to BMP signals. We measured the levels of phosphorylated Mothers against decapentaplegic (pMad), a well-characterized reporter of BMP pathway activation (Figure 5A–E)[15,45]. To control for technical variation in immunofluorescence staining, we then calculated the ratio of nuclear pMad fluorescence intensity values in mutant (GFP-negative) GSCs and adjacent wild-type (GFP-positive) GSCs in the same germarium. In mock mosaics, where all cells are wild-type, GFP-negative and GFP-positive GSCs expressed pMad equivalently (Figure 5E), leading to an average GFP-/GFP+ ratio equal to 0.96 (Figure 5I). Similarly, $Hrb27C^{rF680}$ mutant GSCs also expressed equivalent levels of pMad as adjacent GFP-negative wild-type GSCs (GFP-/GFP+ ratio = 0.92; Figure 5H–I). In contrast, sqd^{ix50} and $heph^{e2}$ mutant GSCs displayed significantly lower levels of nuclear pMad than neighboring wild-type GSCs (Figure 5F–G), resulting in average GFP-GFP+ ratios of 0.53 and 0.79, respectively ($p < 0.0001$; Figure 5I). These data indicate that *sqd* and *heph* are necessary for GSCs to properly respond to niche BMP signals, but that *Hrb27C* likely promotes GSC self-renewal predominately through another mechanism. Taken together, these results suggest that although *Hrb27C*, *sqd*, and *heph* mutant GSCs have reduced capacity for self-renewal, the mechanisms through which these hnRNPs promote self-renewal are likely quite divergent and dependent on regulation of unique sets of transcripts.

DISCUSSION

Gene expression involves the formation of distinct ribonucleoprotein complexes containing nascent transcripts, hnRNPs, and translation initiation factors that regulate the amount and location of protein produced within a cell[46]. Post-transcriptional regulation and translational repression are predominant mechanisms controlling germ cell development, and as such are critical for oogenesis in a variety of organisms[16,17,47–49]. As multifunctional RNA binding proteins, hnRNPs have emerged as important post-transcriptional regulators of gene expression with specialized cellular functions[20]. In *Drosophila* oogenesis, Sqd, Hrb27C, and Glo are necessary for translational repression and localization of *gurken*, *nanos*, and *oskar* mRNAs, whose spatially-regulated translation establishes concentrated areas of asymmetrically distributed protein in the oocyte[23,29,50,51]. Earlier in oogenesis, Hrb98DE promotes GSC self-renewal via regulation of E-cadherin translation[31]; however, it was unknown whether other hnRNPs might also control GSCs. Here, we extend these foundational studies to demonstrate that in addition to their known roles in later stages of oogenesis, three hnRNPs, Hrb27C, Sqd, and Heph, play distinct roles in GSC self-renewal and cyst division and are likely independent of Hrb98DE. Our genetic loss-of-function studies suggest that these hnRNPs individually control unique aspects of GSC and cyst biology, perhaps reflecting unique sets of mRNA targets. Taken together, our study suggests a broad role for hnRNPs in the regulation of GSCs and their daughters.

Our data demonstrate that individual hnRNPs are expressed in a spatially- and temporally-restricted manner in the *Drosophila* germarium. For example, while many hnRNPs are expressed in the germline and soma, Syp is expressed only in somatic cells. Our antibody localization of Syp protein is consistent with recent single-cell RNA sequencing studies demonstrating very low levels of Syp mRNA in mitotically-active germ cells[52,53]. In addition, Heph is highly expressed in mitotically dividing cysts, but its expression decreases in germ cells coincident with the terminal mitotic division. We also find that hnRNPs exhibit distinct intracellular localization. HnRNPs shuttle between the nucleus and the cytoplasm to control the nuclear export of mature mRNAs[46]. Our results demonstrate that NonA and Hrb87F are both concentrated in the nucleus, while Hrb27C appears primarily cytoplasmic. The intracellular location of hnRNPs in germ cells likely reflects their diverse functions in post-transcriptional processing, maturation, and nuclear export of RNA polymerase II-dependent transcripts[54]. For example, NonA preferentially binds introns of nascent RNAs to facilitate nuclear paraspeckle formation (Knott et al., 2016; McMahon et al., 2016), while Hrb27C binds 3’UTRs to control alternative splicing, mRNA localization, and translation (Blanchette et al., 2009; Huynh et al., 2004; McMahon et al., 2016; Nelson et al., 2007).

Attempts to identify transcripts bound by hnRNPs in *Drosophila* have yielded thousands of putative targets and illuminated extensive cross-regulatory interactions[21,55–57]. Our data suggest that Sqd and Heph enable GSCs to properly receive BMP signals. It is tempting to speculate that Sqd and Heph regulate the splicing or stability of essential BMP signaling components autonomous to GSCs, such as the receptors Put or Tkv or the transcription factor Mad. Alternatively, hnRNPs could post-transcriptionally repress factors that normally repress BMP signaling and promote differentiation. Translational repression is critical for the initiation of cyst differentiation[16,17,58]. RNA binding proteins Pumilio (Pum) and

Brain tumor (Brat) post-transcriptionally repress *Mad* and *Med* mRNAs by recruiting the deadenylase complex CCR4-NOT[59,60]. Destabilization of *Mad* and *Med* transcripts by CCR4-NOT aids in repressing BMP signaling in cystoblasts, permitting de-repression of *bam* and other pro-differentiation factors. Pum also forms complexes with Nanos to repress Brat and Mei-P26 in GSCs, suppressing differentiation[59,61,62]. We also cannot exclude a third possibility, that the hnRNPs regulate other as-yet-unidentified transcripts critical for promoting GSC self-renewal. Our finding that Hrb27C promotes GSC proliferation, independent of the reception of BMP signals, suggests that Sqd, Heph, and Hrb27C recognize unique sets of transcripts that contribute to the ability of the GSC to self-renew. Given the extensive repertoire of hnRNPs, and the complexity of the BMP response in GSCs, there is an extremely wide range of putative transcripts that could be regulated by Sqd, Heph, and Hrb27C. Future experiments aimed at elucidating the RNA recognition properties of these hnRNPs may help us understand how they individually regulate GSCs and their dividing daughters.

EXPERIMENTAL PROCEDURES

Drosophila strains and culture conditions

Flies were maintained at 22°−25°C on a standard medium containing cornmeal, molasses, yeast and agar (Nutrify MF; Genesee Scientific) supplemented with yeast. For all experiments, unless otherwise noted, flies were collected 2 to 3 days after eclosion and maintained on standard media at 25°C. Flies were supplemented with wet yeast paste (nutrient-rich diet) 3 days before ovary dissection. Genes/alleles with multiple names are referenced using FlyBase nomenclature (www.flybase.org) for simplicity.

The following alleles were used for protein expression: $Hrb27C^{fTRG00930.sfGFP\text{-}TVPTBF}$ (*Hrb27::GFP*; Vienna #v318283)[44]; $sqd^{CPTI000239}$ (*sqd::GFP*; Kyoto #115104)[63]; *PTB::GFP* (referred to as *Heph::GFP*, a gift of Ilan Davis)[28]; $nonA^{CPTI003091}$ (*nonA::GFP*; Kyoto #115389[63]; $Hrb87F^{CC00189}$ (*Hrb87F::GFP*; a gift of Subhash Lakhotia)[64,65]; and *Bam-sfGFP* (to visualize cytoplasmic Bam; Vienna #v318001)[44].

Genetic mosaic generation, germline RNAi, and stem cell analyses

Genetic mosaic analysis via *Flippase/Flippase Recognition Target* (*Flp/FRT*)[66] used the following alleles on *FRT*-containing chromosomes: sqd^{ix50} and sqd^{ix7724} (gifts of Amanda Norvell); $heph^{e1}$ and $heph^{e237}$ (gifts of William Brook); $Hrb27C^{rF680}$ (gift of Amanda Norvell), $Hrb27C^{K02814}$ (Kyoto #111072), and $Hrb27C^{f04375}$ (Kyoto #114656)[23]. Other genetic tools are described in FlyBase. Genetic mosaics were generated using *FLP/FRT*-mediated recombination in 1–3 day old females carrying a mutant allele *in trans* to a wild-type allele (linked to a *Ubi-GFP* or *NLS-RFP* marker) on homologous *FRT* arms with a *hs-FLP* transgene, as previously described[36]. Flies were heat shocked at 37°C twice per day 6–8 hours apart for 3 days, then incubated at 25°C on standard media supplemented first with dry yeast, then with wet yeast 3 days prior to dissection. Flies were dissected 8 days after clone induction. Wild-type alleles (*FRT40A* or *FRT82B*) were used for control mosaics. GSCs were identified by the location of their fusomes adjacent to the cap cells[40]. GSC loss was measured by the number of germaria that contain a GFP-negative cyst (generated from

the original GFP-negative stem cell) but lack a GFP-negative GSC, compared to the total number of germaria containing a germline clone[36]. Results were analyzed by Chi-square tests comparing GSC loss in mock control germaria (where all cells are wild type) to GSC loss in hnRNP mutant mosaic germaria using Microsoft Excel.

To measure stem cell loss in *P{w$^+$ Tsr$^+$ }/P{w$^+$ Tsr$^+$ }; ry Df(3R)Hrb87F/ry Df(3R)Hrb87F (referred to as Df(3R)Hrb87F)*[39], flies were raised at 25°C and dissected 3, 8, 12, and 21 days after eclosion. GSC loss was measured by the average number of GSCs per germarium in mutants compared to heterozygous sibling controls. Statistical analysis was performed using Student's t-test, in Excel.

For RNAi experiments, germline knock-down was facilitated by expressing the germline-specific *nos-GAL4::VP16-nos.UTR* (referred to throughout as *nos-Gal4::VP16*; Bloomington #4937)[67,68]. Driver expression was confirmed using *UASp-tubGFP* (Bloomington #7373)[69]. Females carrying drivers alone were used as controls. To facilitate sqd knock-down in the germline, the following RNAi lines (carried in *pVALIUM20* or *pVALIUM22* transgenes for maximum germline efficiency) were used: *UAS-sqd^{HMJ21209}* (Bloomington #53891), *sqd^{GL00473}* (Bloomington #35627), and *sqd^{HMC03848}* (Bloomington #55169). For assessing egg laying and egg morphology, 20 pairs of flies of the appropriate genotype (in triplicate) were mated in bottles containing grape agar plates at 37°C for 24 hours. Total numbers of eggs laid and the percentage of dorsalized eggs were quantified by manually counting the eggs under a stereoscope. For counting GSC number, flies were raised at 25°C and dissected 3, 6, and 12 days after eclosion. GSC loss was measured by the average number of GSCs per germarium in mutants compared to driver-only controls. Statistical analysis was performed using Student's unpaired t-test in Excel.

GSC proliferation was measured by counting the number of GFP-negative / EdU-positive GSCs following a one hour incubation in EdU. Chi-squared analysis was used to compare the percentage of total GFP-negative GSCs that also labeled for EdU in mock mosaic germaria versus hnRNP mutant mosaic germaria.

Immunofluorescence and microscopy

Ovaries were dissected, fixed, washed, and blocked as previously described[33,70]. Briefly, ovaries were dissected and teased apart in Grace's media (Lonza or Caisson Labs) and fixed using 5.3% formaldehyde in Grace's media at room temperature for 13 minutes. Ovaries were washed extensively in phosphate-buffered saline (PBS, pH 7.4; Thermo Fisher) with 0.1% Triton X-100, then blocked for three hours in a blocking solution consisting of 5% bovine serum albumin (Sigma), 5% normal goat serum (MP Biomedicals) and 0.1% Triton-X-100 in PBS. The following primary antibodies were diluted in block and used overnight at 4°C: mouse anti-Lamin C (LamC) [LC28.26, Developmental Studies Hybridoma Bank (DSHB), 1:100], mouse anti-Hts (1B1, DSHB, 1:10), rabbit anti-GFP (ab6556, Abcam, 1:2000), chicken anti-GFP (ab13970, Abcam, 1:2000), guinea pig anti-Syncrip (a gift from I. Davis, 1:5000)[35], rabbit anti-cleaved Caspase 3 (9661, Cell Signaling Technology, 1:50), rat anti-E-cadherin (DCAD2, DSHB, 1:20), rabbit anti-pMad [(Smad3) phospho S423 + S425, ab52903, Abcam/Epitomics, 1:50]. Samples incubated with pMad were permeabilized with 0.5% Triton-X100 in PBS for thirty minutes before blocking. Samples were incubated

with Alexa Fluor 488-, 568- or 633-conjugated goat-species specific secondary antibodies (Molecular Probes; 1:200). EdU was detected using AlexaFluor-594 or −647 via Click-It chemistry following the manufacturer's recommendations (Life Technologies) and counterstained with DAPI (Sigma 1:1000 in PBS). Ovaries were then mounted in 90% glycerol containing 20.0 μg/mL N-propyl gallate (Sigma). Data was collected using a Zeiss LSM 700 laser scanning confocal microscope. Images were analyzed using Zen Blue 2012 software and images were minimally and equally enhanced via histogram using Zen and Adobe Photoshop CC.

Quantification of fluorescence intensity in GSCs

Fluorescence intensity in confocal sections was measured via ZEN Blue 2012 (Zeiss) by manually demarcating individual GSC and measuring nuclear intensity mean values (IMV; gray value/pixel) at the z-level containing the largest nuclear diameter for the specific antibody analyzed. Because of slight variations in pixel intensity among stain sets, IMVs for each fluorescent protein were calculated for a minimum of 30 individual GSCs. Controls are adjacent GFP-positive (wild type) GSCs within the same germarium. To normalize pMAD quantification, IMVs were evaluated as a ratio of GFP-/GFP+ GSCs within the same germarium, where a ratio equal to 1.0 represented equivalent intensity in both cells. Statistical analysis was performed using Student's unpaired two-tailed T-test with Mann-Whitney nonparametric post-test using Prism (GraphPad).

ACKNOWLEDGMENTS

Many thanks to: D. Drummond-Barbosa, A. Norvell, T. Schüpbach, W. Brook, I. Davis, P. Lasko, the Bloomington, Vienna, and Kyoto *Drosophila* Stock Centers, and the Developmental Studies Hybridoma Bank for fly stocks and antibodies; the ECU Department of Biology Genomics and Microscopy Core Facilities; and A. Norvell, B. Thompson, C. Geyer, B. Capel, J.-L. Scemama, members of the Ables laboratory, and our anonymous reviewers for helpful discussions and critical reading of this manuscript.

FUNDING

This work was supported by National Institutes of Health R15 GM117502 (E.T.A.), March of Dimes Basil O'Connor Research Starter Award 5-FY14-62 (E.T.A.), Sigma Xi Grant-in-Aid of Research (D.S.F.), and the East Carolina University (ECU) Division of Research and Graduate Studies and Thomas Harriot College of Arts and Sciences (E.T.A.). A.E.W. was supported by the ECU Office of Undergraduate Research. V.V.H. was supported by the ECU Office of Undergraduate Research, ECU Honors College, and the EC Scholars Program.

REFERENCES

1. Gervais L, Bardin AJ. Tissue homeostasis and aging: new insight from the fly intestine. Current opinion in cell biology. Oct 2017;48:97–105. 10.1016/j.ceb.2017.06.005. [PubMed: 28719867]
2. Ge Y, Fuchs E. Stretching the limits: from homeostasis to stem cell plasticity in wound healing and cancer. Nature reviews Genetics. May 2018;19(5):311–325. 10.1038/nrg.2018.9.
3. Chen C, Fingerhut JM, Yamashita YM. The ins(ide) and outs(ide) of asymmetric stem cell division. Current opinion in cell biology. Dec 2016;43:1–6. 10.1016/j.ceb.2016.06.001. [PubMed: 27318429]
4. Pan L, Chen S, Weng C, et al. Stem cell aging is controlled both intrinsically and extrinsically in the Drosophila ovary. Cell Stem Cell. Oct 11 2007;1(4):458–69. 10.1016/j.stem.2007.09.010. [PubMed: 18371381]
5. Oh J, Lee YD, Wagers AJ. Stem cell aging: mechanisms, regulators and therapeutic opportunities. Nature medicine. Aug 2014;20(8):870–80. 10.1038/nm.3651.
6. Keyes BE, Fuchs E. Stem cells: Aging and transcriptional fingerprints. The Journal of Cell Biology. 2018;217(1):79–92. 10.1083/jcb.201708099. [PubMed: 29070608]

7. McLaughlin JM, Bratu DP. Drosophila melanogaster Oogenesis: An Overview. Methods in molecular biology (Clifton, NJ). 2015;1328:1–20. 10.1007/978-1-4939-2851-4_1.
8. Drummond-Barbosa D Local and Physiological Control of Germline Stem Cell Lineages in Drosophila melanogaster. Genetics. Sep 2019;213(1):9–26. 10.1534/genetics.119.300234. [PubMed: 31488592]
9. Hinnant TD, Merkle JA, Ables ET. Coordinating Proliferation, Polarity, and Cell Fate in the Drosophila Female Germline. Front Cell Dev Biol. 2020;8:19. 10.3389/fcell.2020.00019. [PubMed: 32117961]
10. Xie T Control of germline stem cell self-renewal and differentiation in the Drosophila ovary: concerted actions of niche signals and intrinsic factors. Wiley interdisciplinary reviews Developmental biology. Mar-Apr 2013;2(2):261–73. 10.1002/wdev.60. [PubMed: 24009036]
11. Xie T, Spradling AC. decapentaplegic is essential for the maintenance and division of germline stem cells in the Drosophila ovary. Cell. Jul 24 1998;94(2):251–60. [PubMed: 9695953]
12. Song X, Zhu CH, Doan C, Xie T. Germline stem cells anchored by adherens junctions in the Drosophila ovary niches. Science. Jun 7 2002;296(5574):1855–7. 10.1126/science.1069871. [PubMed: 12052957]
13. Chen D, McKearin D. Dpp signaling silences bam transcription directly to establish asymmetric divisions of germline stem cells. Current Biology. 2003;13(20):1786–1791. [PubMed: 14561403]
14. McKearin D, Ohlstein B. A role for the Drosophila bag-of-marbles protein in the differentiation of cystoblasts from germline stem cells. Development. 1995;121(9):2937–2947. [PubMed: 7555720]
15. Song X, Wong MD, Kawase E, et al. Bmp signals from niche cells directly repress transcription of a differentiation-promoting gene, bag of marbles, in germline stem cells in the Drosophila ovary. Development. 2004;131(6):1353–1364. [PubMed: 14973291]
16. Blatt P, Martin ET, Breznak SM, Rangan P. Post-transcriptional gene regulation regulates germline stem cell to oocyte transition during Drosophila oogenesis. Curr Top Dev Biol. 2020;140:3–34. 10.1016/bs.ctdb.2019.10.003. [PubMed: 32591078]
17. Slaidina M, Lehmann R. Translational control in germline stem cell development. The Journal of Cell Biology. 2014;207(1):13–21. 10.1083/jcb.201407102. [PubMed: 25313405]
18. Chaudhury A, Chander P, Howe PH. Heterogeneous nuclear ribonucleoproteins (hnRNPs) in cellular processes: Focus on hnRNP E1's multifunctional regulatory roles. RNA (New York, NY). Aug 2010;16(8):1449–62. 10.1261/rna.2254110.
19. Jean-Philippe J, Paz S, Caputi M. hnRNP A1: the Swiss army knife of gene expression. Int J Mol Sci. Sep 16 2013;14(9):18999–9024. 10.3390/ijms140918999. [PubMed: 24065100]
20. Piccolo LL, Corona D, Onorati MC. Emerging Roles for hnRNPs in post-transcriptional regulation: what can we learn from flies? Chromosoma. Dec 2014;123(6):515–27. 10.1007/s00412-014-0470-0. [PubMed: 24913828]
21. Blanchette M, Green RE, MacArthur S, et al. Genome-wide analysis of alternative pre-mRNA splicing and RNA-binding specificities of the Drosophila hnRNP A/B family members. Mol Cell. Feb 27 2009;33(4):438–49. 10.1016/j.molcel.2009.01.022. [PubMed: 19250905]
22. Singh R, Valcárcel J. Building specificity with nonspecific RNA-binding proteins. Nat Struct Mol Biol. Aug 2005;12(8):645–53. 10.1038/nsmb961. [PubMed: 16077728]
23. Goodrich JS, Clouse KN, Schupbach T. Hrb27C, Sqd and Otu cooperatively regulate gurken RNA localization and mediate nurse cell chromosome dispersion in Drosophila oogenesis. Development. May 2004;131(9):1949–58. 10.1242/dev.01078. [PubMed: 15056611]
24. Kelley RL. Initial organization of the Drosophila dorsoventral axis depends on an RNA-binding protein encoded by the squid gene. Genes & Development. June 1, 1993 1993;7(6):948–960. 10.1101/gad.7.6.948. [PubMed: 7684991]
25. Matunis EL, Kelley R, Dreyfuss G. Essential role for a heterogeneous nuclear ribonucleoprotein (hnRNP) in oogenesis: hrp40 is absent from the germ line in the dorsoventral mutant squid. Proceedings of the National Academy of Sciences. 1994;91(7):2781–2784.
26. Norvell A, Kelley RL, Wehr K, Schupbach T. Specific isoforms of squid, a Drosophila hnRNP, perform distinct roles in Gurken localization during oogenesis. Genes Dev. Apr 1 1999;13(7):864–76. [PubMed: 10197986]

27. Steinhauer J, Kalderon D. The RNA-binding protein Squid is required for the establishment of anteroposterior polarity in the Drosophila oocyte. Development. Dec 2005;132(24):5515–25. 10.1242/dev.02159. [PubMed: 16291786]
28. Besse F, Lopez de Quinto S, Marchand V, Trucco A, Ephrussi A. Drosophila PTB promotes formation of high-order RNP particles and represses oskar translation. Genes Dev. Jan 15 2009;23(2):195–207. 10.1101/gad.505709. [PubMed: 19131435]
29. Huynh J-R, Munro TP, Smith-Litière K, Lepesant J-A, Johnston DS. The Drosophila hnRNPA/B Homolog, Hrp48, Is Specifically Required for a Distinct Step in osk mRNA Localization. Developmental Cell. 5// 2004;6(5):625–635. 10.1016/S1534-5807(04)00130-3. [PubMed: 15130488]
30. Yano T, De Quinto SL, Matsui Y, Shevchenko A, Shevchenko A, Ephrussi A. Hrp48, a Drosophila hnRNPA/B Homolog, Binds and Regulates Translation of oskar mRNA. Developmental Cell. 2004;6(5):637–648. [PubMed: 15130489]
31. Ji Y, Tulin AV. Poly(ADP-ribose) controls DE-cadherin-dependent stem cell maintenance and oocyte localization [10.1038/ncomms1759]. Nat Commun. 03/27/online 2012;3:760. https://doi.orghttp://www.nature.com/ncomms/journal/v3/n3/suppinfo/ncomms1759_S1.html. [PubMed: 22453833]
32. Xie W, Zhu H, Zhao M, et al. Crucial roles of different RNA-binding hnRNP proteins in Stem Cells. Int J Biol Sci. 2021;17(3):807–817. 10.7150/ijbs.55120. [PubMed: 33767590]
33. Ables ET, Hwang GH, Finger DS, Hinnant TD, Drummond-Barbosa D. A Genetic Mosaic Screen Reveals Ecdysone-Responsive Genes Regulating Drosophila Oogenesis. G3 (Bethesda, Md). Aug 09 2016;6(8):2629–42. 10.1534/g3.116.028951. [PubMed: 27226164]
34. Yan D, Neumüller RA, Buckner M, et al. A regulatory network of Drosophila germline stem cell self-renewal. Developmental cell. 2014;28(4):459–473. 10.1016/j.devcel.2014.01.020. [PubMed: 24576427]
35. McDermott SM, Meignin C, Rappsilber J, Davis I. Drosophila Syncrip binds the gurken mRNA localisation signal and regulates localised transcripts during axis specification. Biology Open. 2012;1(5):488–497. 10.1242/bio.2012885. [PubMed: 23213441]
36. Laws KM, Drummond-Barbosa D. Genetic Mosaic Analysis of Stem Cell Lineages in the Drosophila Ovary. Methods in molecular biology (Clifton, NJ). 2015;1328:57–72. 10.1007/978-1-4939-2851-4_4.
37. Dansereau DA, Lunke MD, Finkielsztein A, Russell MA, Brook WJ. hephaestus encodes a polypyrimidine tract binding protein that regulates Notch signalling during wing development in Drosophila melanogaster. Development. December 15, 2002 2002;129(24):5553–5566. 10.1242/dev.00153. [PubMed: 12421697]
38. Hammond LE, Rudner DZ, Kanaar R, Rio DC. Mutations in the hrp48 gene, which encodes a Drosophila heterogeneous nuclear ribonucleoprotein particle protein, cause lethality and developmental defects and affect P-element third-intron splicing in vivo. Molecular and Cellular Biology. 1997;17(12):7260–7267. [PubMed: 9372958]
39. Singh AK, Lakhotia SC. The hnRNP A1 homolog Hrp36 is essential for normal development, female fecundity, omega speckle formation and stress tolerance in Drosophila melanogaster [journal article]. Journal of Biosciences. September 01 2012;37(4):659–678. 10.1007/s12038-012-9239-x. [PubMed: 22922191]
40. de Cuevas M, Spradling AC. Morphogenesis of the Drosophila fusome and its implications for oocyte specification. Development. 1998;125(15):2781–2789. [PubMed: 9655801]
41. Ong S, Tan C. Germline cyst formation and incomplete cytokinesis during Drosophila melanogaster oogenesis. Dev Biol. Jan 1 2010;337(1):84–98. 10.1016/j.ydbio.2009.10.018. [PubMed: 19850028]
42. Ni JQ, Zhou R, Czech B, et al. A genome-scale shRNA resource for transgenic RNAi in Drosophila. Nat Methods. May 2011;8(5):405–7. 10.1038/nmeth.1592. [PubMed: 21460824]
43. DeLuca SZ, Spradling AC. Efficient Expression of Genes in the Drosophila Germline Using a UAS Promoter Free of Interference by Hsp70 piRNAs. Genetics. Jun 2018;209(2):381–387. 10.1534/genetics.118.300874. [PubMed: 29669732]

44. Sarov M, Barz C, Jambor H, et al. A genome-wide resource for the analysis of protein localisation in Drosophila. eLife. Feb 20 2016;5:e12068. 10.7554/eLife.12068. [PubMed: 26896675]
45. Kai T, Spradling A. An empty Drosophila stem cell niche reactivates the proliferation of ectopic cells. Proceedings of the National Academy of Sciences of the United States of America. Apr 15 2003;100(8):4633–8. 10.1073/pnas.0830856100. [PubMed: 12676994]
46. Bjork P, Wieslander L. Integration of mRNP formation and export. Cellular and molecular life sciences : CMLS. Aug 2017;74(16):2875–2897. 10.1007/s00018-017-2503-3. [PubMed: 28314893]
47. Jin L, Neiman AM. Post-transcriptional regulation in budding yeast meiosis. Current genetics. May 2016;62(2):313–5. 10.1007/s00294-015-0546-2. [PubMed: 26613728]
48. Licatalosi DD. Roles of RNA-binding Proteins and Post-transcriptional Regulation in Driving Male Germ Cell Development in the Mouse. Advances in experimental medicine and biology. 2016;907:123–51. 10.1007/978-3-319-29073-7_6. [PubMed: 27256385]
49. Nousch M, Eckmann CR. Translational control in the Caenorhabditis elegans germ line. Advances in experimental medicine and biology. 2013;757:205–47. 10.1007/978-1-4614-4015-4_8. [PubMed: 22872479]
50. Kalifa Y, Huang T, Rosen LN, Chatterjee S, Gavis ER. Glorund, a Drosophila hnRNP F/H Homolog, Is an Ovarian Repressor of nanos Translation. Developmental Cell. 2006/03/01/ 2006;10(3):291–301. https://doi.org10.1016/j.devcel.2006.01.001. [PubMed: 16516833]
51. Kalifa Y, Armenti ST, Gavis ER. Glorund interactions in the regulation of gurken and oskar mRNAs. Developmental biology. 11/05 2009;326(1):68–74. 10.1016/j.ydbio.2008.10.032. [PubMed: 19013444]
52. Martin ET, Sarkar K, McCarthy A, Rangan P. Oo-site: A dashboard to visualize gene expression during Drosophila oogenesis suggests meiotic entry is regulated post-transcriptionally. Biol Open. May 15 2022;11(5). 10.1242/bio.059286.
53. Slaidina M, Gupta S, Banisch TU, Lehmann R. A single-cell atlas reveals unanticipated cell type complexity in Drosophila ovaries. Genome research. Oct 2021;31(10):1938–1951. 10.1101/gr.274340.120. [PubMed: 34389661]
54. Levengood JD, Tolbert BS. Idiosyncrasies of hnRNP A1-RNA recognition: Can binding mode influence function. Seminars in cell & developmental biology. Apr 9 2018. 10.1016/j.semcdb.2018.04.001.
55. Brooks AN, Duff MO, May G, et al. Regulation of alternative splicing in Drosophila by 56 RNA binding proteins. Genome research. Nov 2015;25(11):1771–80. 10.1101/gr.192518.115. [PubMed: 26294686]
56. McMahon Aoife C, Rahman R, Jin H, et al. TRIBE: Hijacking an RNA-Editing Enzyme to Identify Cell-Specific Targets of RNA-Binding Proteins. Cell. 2016/04/21/ 2016;165(3):742–753. https://doi.org10.1016/j.cell.2016.03.007. [PubMed: 27040499]
57. Stoiber MH, Olson S, May GE, et al. Extensive cross-regulation of post-transcriptional regulatory networks in Drosophila. Genome research. Nov 2015;25(11):1692–702. 10.1101/gr.182675.114. [PubMed: 26294687]
58. Mercer M, Jang S, Ni C, Buszczak M. The Dynamic Regulation of mRNA Translation and Ribosome Biogenesis During Germ Cell Development and Reproductive Aging. Front Cell Dev Biol. 2021;9:710186. 10.3389/fcell.2021.710186. [PubMed: 34805139]
59. Joly W, Chartier A, Rojas-Rios P, Busseau I, Simonelig M. The CCR4 deadenylase acts with Nanos and Pumilio in the fine-tuning of Mei-P26 expression to promote germline stem cell self-renewal. Stem cell reports. 2013;1(5):411–24. 10.1016/j.stemcr.2013.09.007. [PubMed: 24286029]
60. Newton FG, Harris RE, Sutcliffe C, Ashe HL. Coordinate post-transcriptional repression of Dpp-dependent transcription factors attenuates signal range during development. Development. Oct 1 2015;142(19):3362–73. 10.1242/dev.123273. [PubMed: 26293305]
61. Li Y, Zhang Q, Carreira-Rosario A, Maines JZ, McKearin DM, Buszczak M. Mei-p26 cooperates with Bam, Bgcn and Sxl to promote early germline development in the Drosophila ovary. PLoS One. 2013;8(3):e58301. 10.1371/journal.pone.0058301. [PubMed: 23526974]

62. Neumuller RA, Betschinger J, Fischer A, et al. Mei-P26 regulates microRNAs and cell growth in the Drosophila ovarian stem cell lineage. Nature. Jul 10 2008;454(7201):241–5. 10.1038/nature07014. [PubMed: 18528333]

63. Lye CM, Naylor HW, Sanson B. Subcellular localisations of the CPTI collection of YFP-tagged proteins in Drosophila embryos. Development. Oct 2014;141(20):4006–17. 10.1242/dev.111310. [PubMed: 25294944]

64. Buszczak M, Paterno S, Lighthouse D, et al. The carnegie protein trap library: a versatile tool for Drosophila developmental studies. Genetics. Mar 2007;175(3):1505–31. 10.1534/genetics.106.065961. [PubMed: 17194782]

65. Singh AK, Lakhotia SC. Dynamics of hnRNPs and omega speckles in normal and heat shocked live cell nuclei of Drosophila melanogaster. Chromosoma. Sep 2015;124(3):367–83. 10.1007/s00412-015-0506-0. [PubMed: 25663367]

66. Xu T, Rubin GM. The effort to make mosaic analysis a household tool. Development. Dec 2012;139(24):4501–3. 10.1242/dev.085183. [PubMed: 23172911]

67. Rørth P Gal4 in the Drosophila female germline. Mech Dev. Nov 1998;78(1–2):113–8. 10.1016/s0925-4773(98)00157-9. [PubMed: 9858703]

68. Van Doren M, Williamson AL, Lehmann R. Regulation of zygotic gene expression in Drosophila primordial germ cells. Current biology : CB. Feb 12 1998;8(4):243–6. 10.1016/s0960-9822(98)70091-0. [PubMed: 9501989]

69. Grieder NC, de Cuevas M, Spradling AC. The fusome organizes the microtubule network during oocyte differentiation in Drosophila. Development. Oct 2000;127(19):4253–64. 10.1242/dev.127.19.4253. [PubMed: 10976056]

70. Hinnant TD, Alvarez AA, Ables ET. Temporal remodeling of the cell cycle accompanies differentiation in the Drosophila germline. Developmental Biology. 2017/09/01/ 2017;429(1):118–131. 10.1016/j.ydbio.2017.07.001. [PubMed: 28711427]

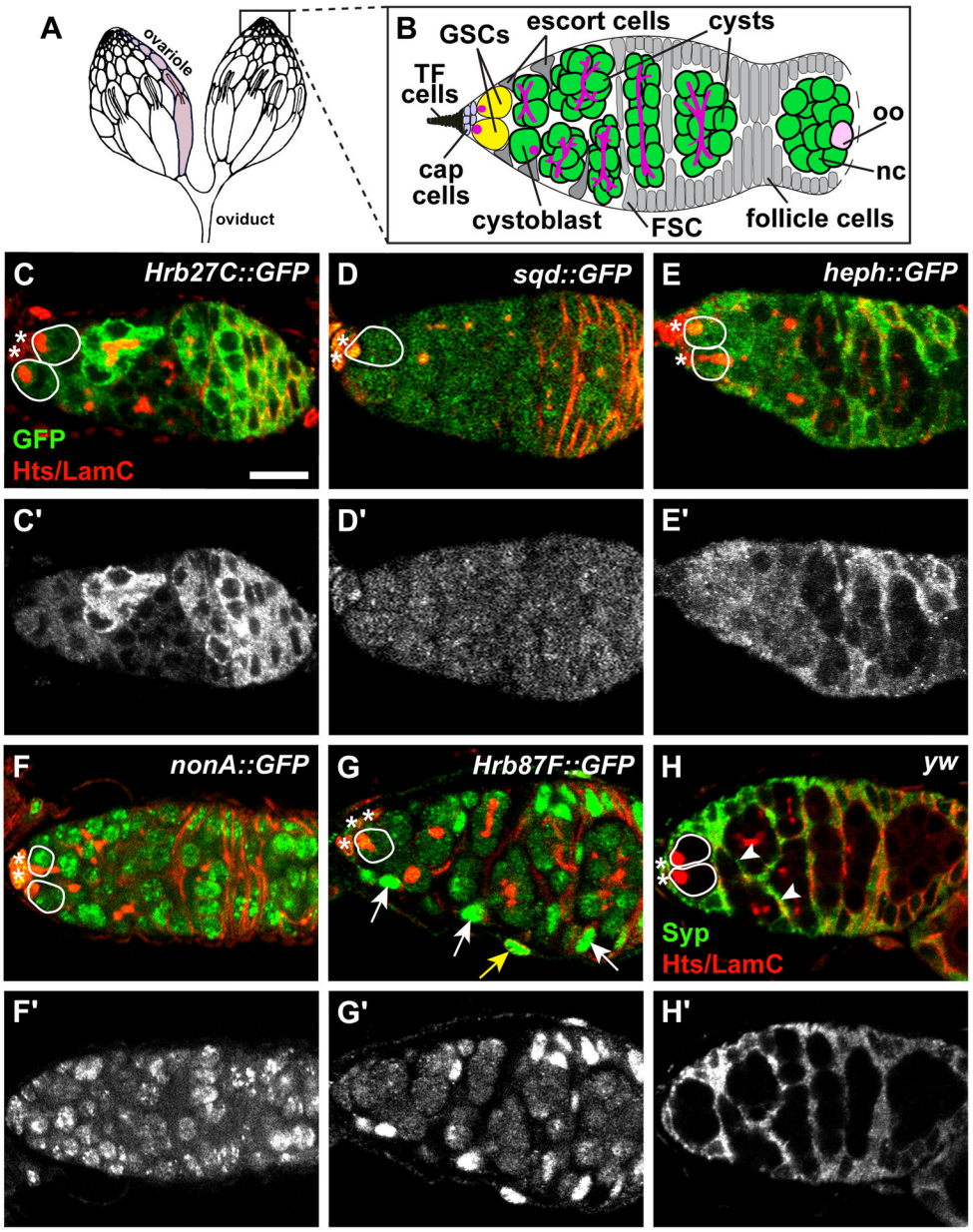

Figure 1.

Drosophila hnRNPs are expressed in distinct patterns in the germarium. (A-B) The ovary (A) is composed of 15–20 ovarioles (one ovariole is shaded in light gray). At the anterior tip of each ovariole is a germarium (B), where germline stem cells (GSCs; yellow) are anchored to a somatic niche (light blue) composed of cap cells and terminal filament (TF) cells. GSCs divide asymmetrically to form cystoblasts (green) which divide mitotically four times with incomplete cytokinesis, forming cysts (green). One cell in the cyst becomes the oocyte (oo, pink); the other 15 become nurse cells (nc, green). Germ cells are characterized by the presence of a fusome (magenta), which extends as germ cells divide. Somatic escort cells (gray triangles) signal to germ cells to promote differentiation. Follicle stem cells (FSC; gray) give rise to follicle cells (gray) which surround the 16-cell germline cyst,

giving rise to an egg chamber that buds off the germarium. (C-H) Representative germaria from GFP-tagged hnRNP transgenic flies labeled with anti-GFP (C-G) or wild-type flies labeled anti-Syp (H) and counterstained with anti-Hts+anti-LamC (red; fusomes, follicle cell membranes, and cap cell nuclear envelopes). Grayscale images of the corresponding green channel alone in C'-H'. Solid white lines demarcate GSCs; asterisks represent cap cells. Somatic cell nuclei (arrows) or membrane extensions (arrowheads) are indicated in G-H. The yellow arrow in G points to an ovarian sheath cell nucleus. Scale bar = 10 μm.

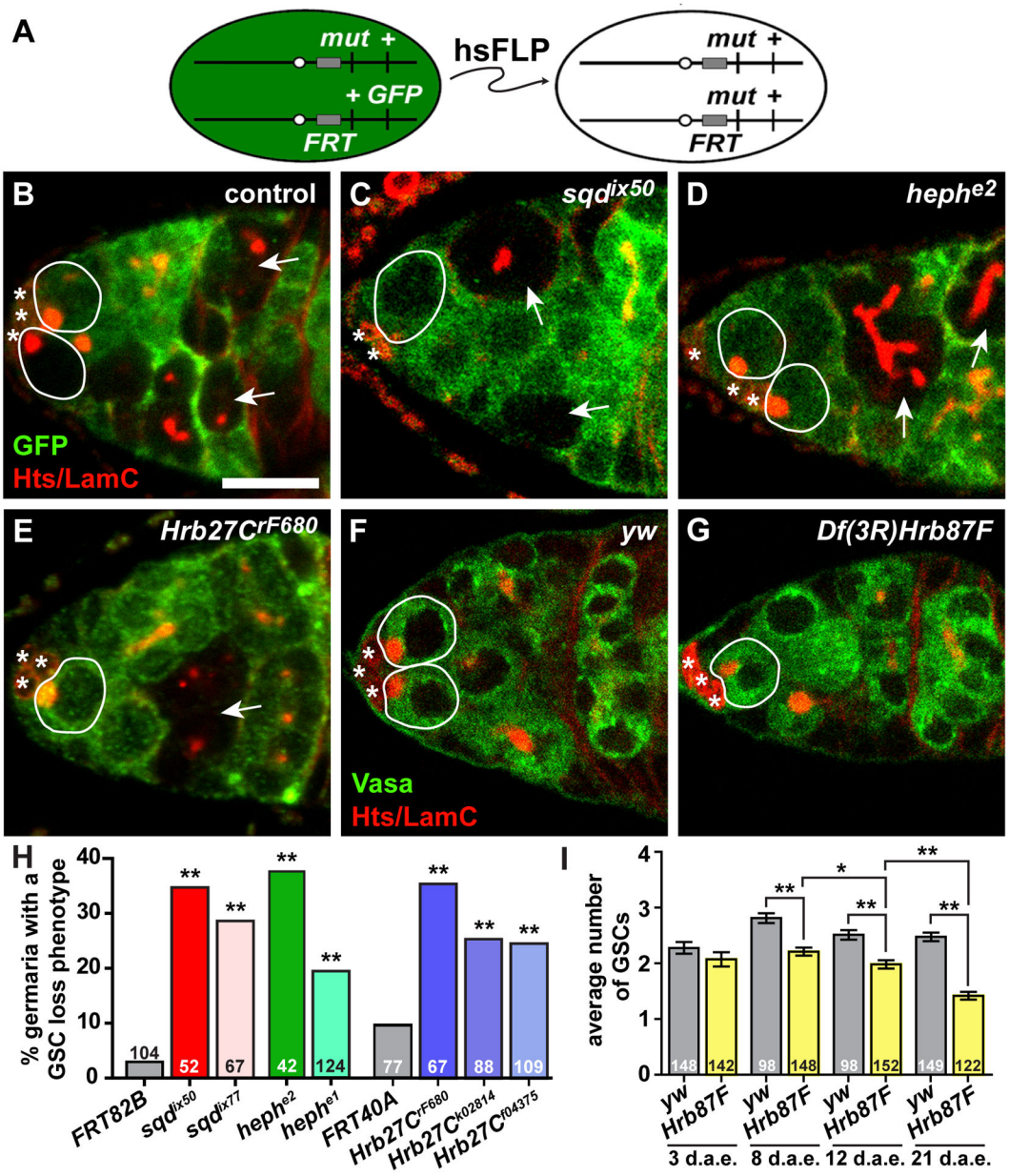

Figure 2.

HnRNPs are required for GSC self-renewal. (A) The FLP/FRT technique was used to generate genetic mosaics. Mitotic recombination is mediated by heat-shock-induced expression of flippase (hsFLP). Homozygous mutant (mut) cells are identified by the absence of a GFP marker, which is linked to the wild-type allele. (B-E) Mock mosaic control (B), sqdix50 (C), hephe2 (D), or Hrb27CrF680 (E) mutant mosaic germaria labeled with anti-GFP (green; wild-type cells) and anti-Hts+anti-LamC (red; fusomes, follicle cell membranes, and cap cell nuclear envelopes). GSCs are outlined in white (wild-type = solid line; mutant = dashed line); asterisks indicate cap cells. Arrows indicate GFP-negative cysts. Scale bar = 5 μm. (F-G) Sibling control (F) or Df(3L)Hrb87F mutant germaria labeled with

anti-Vasa (green; germ cells), anti-Hts (red), and anti-LamC (red). GSCs are outlined. (H) *p < 0.05, **p < 0.001; Chi-squares test (F, H) or Student's two-tailed T-test (G)

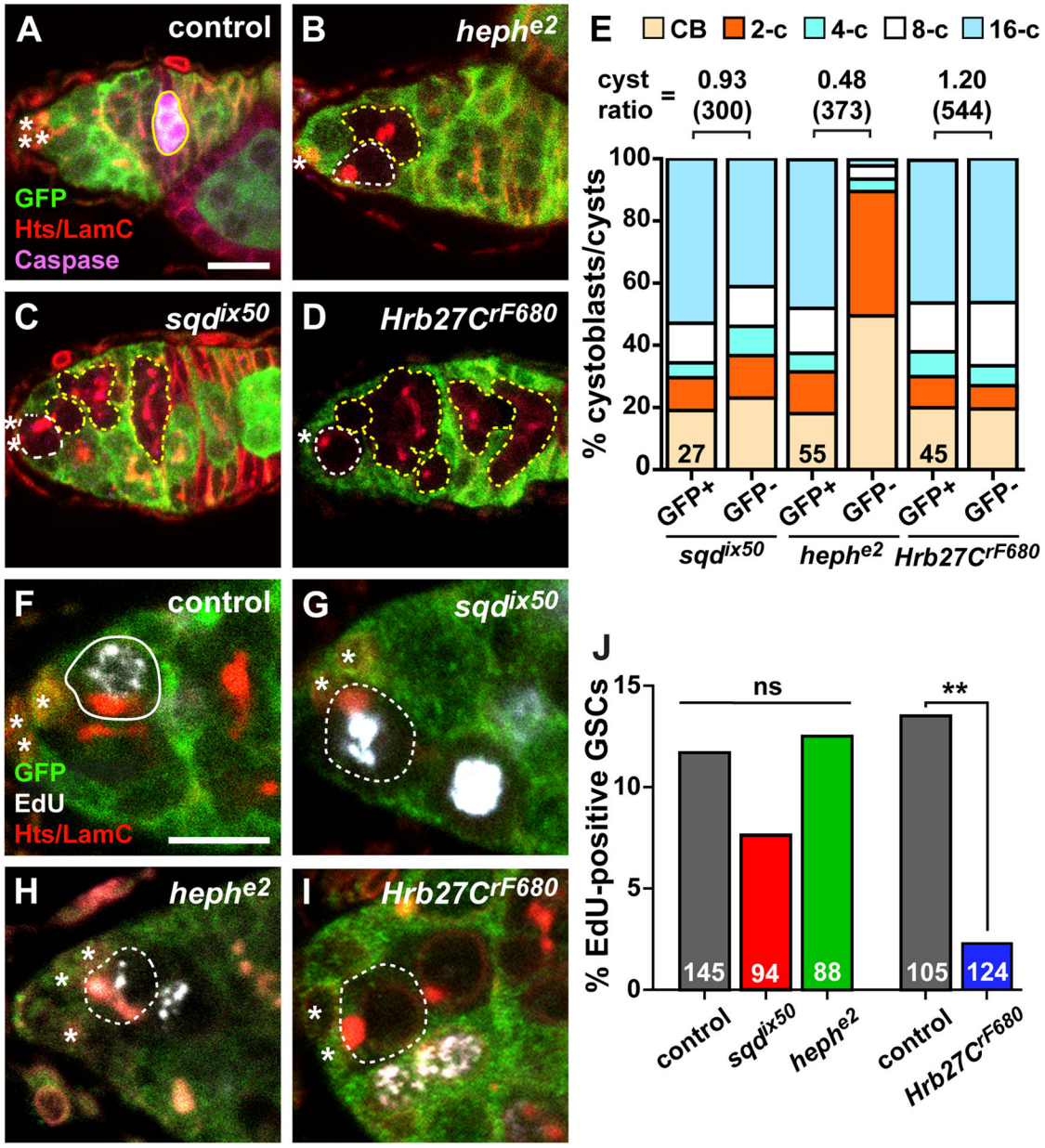

Figure 3.

Heph and Hrb27C are necessary for timely cyst divisions and GSC proliferation, respectively. (A-D) Mock mosaic germarium from a female raised on a nutrient-deficient diet (control, A), hephe2 (B), sqdix50 (C), and Hrb27CrF680 (D) mosaic germaria stained with anti-GFP (green; wild-type cells), anti-cleaved Caspase (magenta, dying cysts), anti-Hts+anti-LamC (red; fusomes, follicle cell membranes, and cap cell nuclear envelopes). Since germaria from wild-type flies raised on nutrient-rich media rarely have dying cysts, a nutrient-deficient diet was used for one set of controls to ensure staining conditions for the cleaved-Caspase antibody were sufficient. (E) Percentage of total control (GFP+) or mutant (GFP-) cystoblasts/cysts in hnRNP mosaic germaria. Numbers in bars represent number of germline-mosaic germaria analyzed. Cyst division ratios are listed above bars

(number of cysts scored in parentheses). (F-I) Mock mosaic (F), sqdix50 (G), hephe2 (H), and Hrb27CrF680 (I) mosaic germaria stained with anti-GFP (green; wild-type cells), EdU (white; cells in S phase), anti-Hts+anti-LamC (red). (J) Percentage of GFP-negative GSCs that are positive for EdU in mosaic germaria eight days after heat shock. Numbers in bars represent the number of GFP-negative GSCs analyzed. **$p < 0.001$, Chi-squares test. GSCs are outlined in white and cystoblasts/cysts are outlined in yellow (wild-type = solid line; mutant = dashed line); asterisks indicate cap cells. A caspase-positive wild-type cyst is outlined in yellow in A. Scale bars = 5 μm

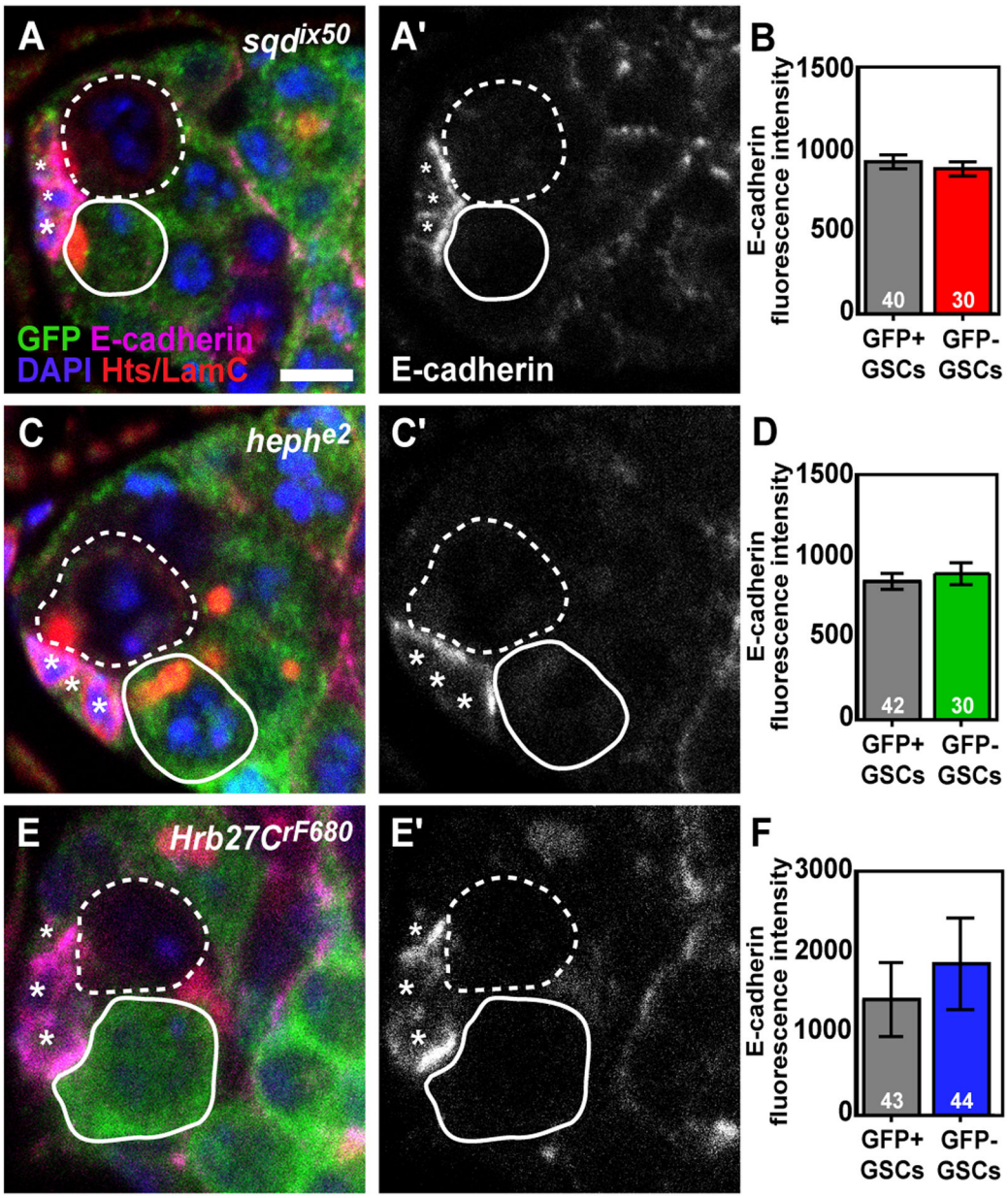

Figure. 4.

Loss of Hrb27C, sqd, or heph does not impact E-cadherin levels at the GSC/Cap cell interface. (A, C, E) sqdix50 (A), hephe2 (C), and Hrb27CrF680 (E) mosaic germaria labeled with anti-GFP (green, wild-type cells), anti-E-cadherin (magenta), anti-Hts+anti-LamC (red; fusomes, follicle cell membranes, and cap cell nuclear envelopes), and DAPI (blue; DNA). Greyscale images of E-cadherin alone are shown in A', C', and E'. GSCs are outlined in white (wild-type = solid line; mutant = dashed line), asterisks indicate cap cells. (B, D, F). Fluorescence intensity mean value (IMV) of E-cadherin antibody labeling in adjacent control (wild-type; GFP+) and mutant (GFP-) GSCs in sqdix50 (B), hephe2 (D), and Hrb27CrF680 (F) mosaic germaria. Error bars, mean ± SEM. Numbers in bars represent the number of GSCs analyzed. Scale bar = 5 μm

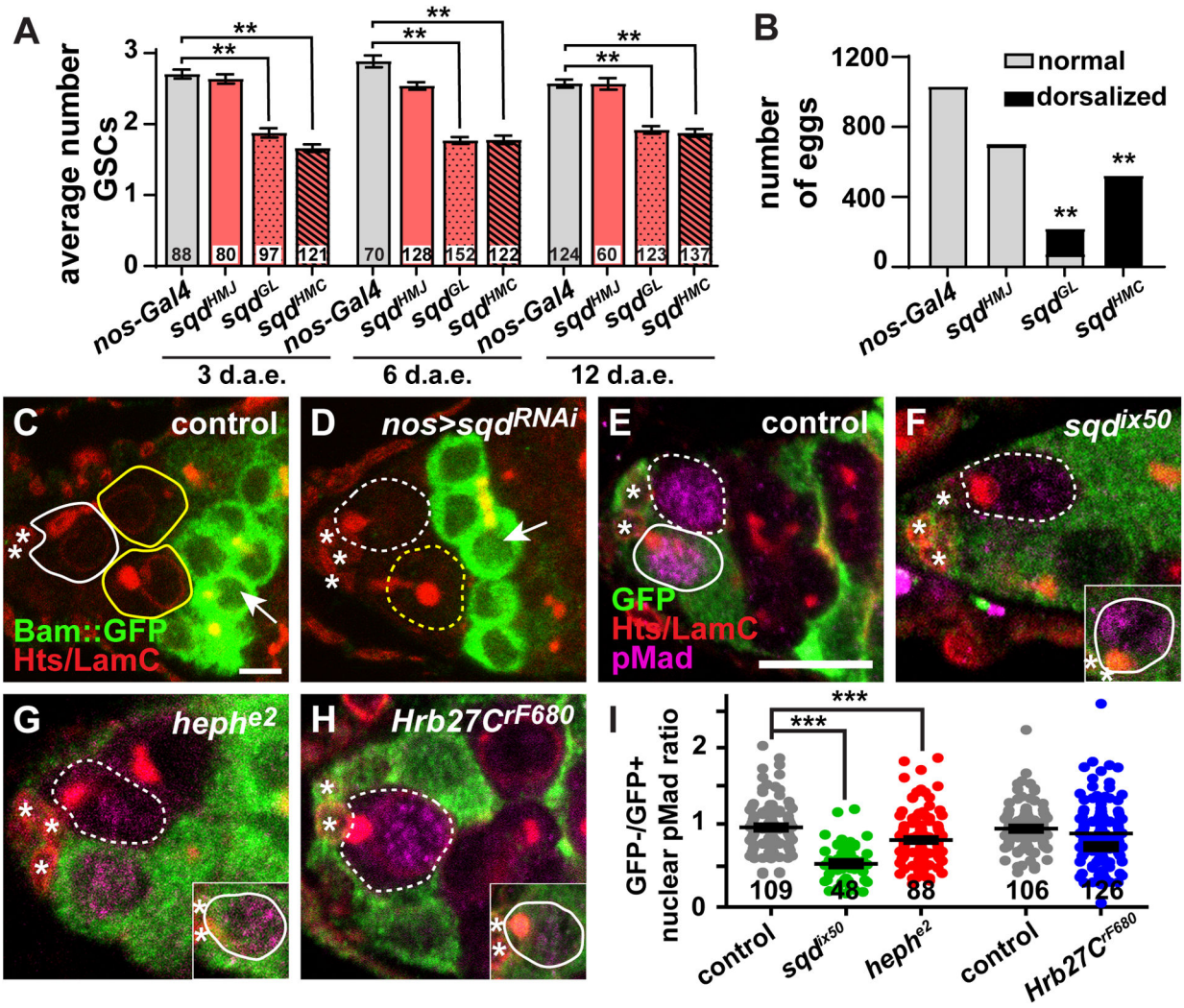

Figure 5.

heph and sqd mutant GSCs have a reduced response to BMP signals. (A) Average number of GSCs per germarium at 3, 6, and 12 days after eclosion in nos-Gal4::VP16 control (gray) or nos-Gal4::VP16>sqd RNAi (light red). Error bars, mean ± SEM. Numbers in bars represent number of germaria analyzed. (B) Total normal (gray) or dorsalized (black) eggs laid by nos-Gal4::VP16 control or nos-Gal4::VP16>sqd RNAi females. **p < 0.001; Student's two-tailed T-test. (C-D) Driver control (C) or nos-Gal4::VP16>sqdGL RNAi (D) germaria expressing Bam-sfGFP in germaria labeled with anti-GFP (green) and anti-Hts+anti-LamC (red). Arrows indicate 4-cell cysts. (E-H) Single z-plane images of mock mosaic (E), sqdix50 (F), hephe2 (G), and Hrb27CrF680 (H) mosaic germaria labeled with anti-GFP (green, wild-type cells), anti-pMad (magenta), and anti-Hts+anti-LamC (red; fusomes, follicle cell membranes, and cap cell nuclear envelopes). A GFP+ wild-type GSC from the same germarium (but in a different z-plane) is shown in insets (F-H). (I) Ratio of GFP- to GFP+ fluorescence intensity mean value of anti-pMAD antibody labeling in GSCs within the same germarium. Each dot represents one GSC pair. ***p < 0.0001; Student's two-tailed T-test with Mann-Whitney non-parametric post-test. Error bars, mean ± SEM.

Number of germaria analyzed below dots. GSCs are outlined in white and cystoblasts/cysts are outlined in yellow (wild-type = solid line; mutant = dashed line); asterisks indicate cap cells. Scale bars = 10 μm (E-H) or 5 μm (C-D)